PAPER

Check for updates

Accessing trifluoromethylated SuFEx-able pyrazole *via* distortion-accelerated 1,3-dipolar cycloadditions

Bipin Khanal, [a] Mark Aldren M. Feliciano [b] and Brian Gold *[a]

Fluorinated pyrazoles are valuable scaffolds with wide-ranging applications in medicinal chemistry, agrochemistry and materials science. We report the 1,3-dipolar cycloaddition of 2,2,2-trifluorodiazoethane and 1-bromoethene-1-sulfonyl fluoride for the concise synthesis of 5-(trifluoromethyl)-1*H*-pyrazole-3-sulfonyl fluoride. Computational analysis revealed that lowered distortion energies account for increased reactivity relative to other stabilized diazo compounds. The resulting trifluoromethylated pyrazole contains a SuFEx-able click handle, enabling orthogonal diversification pathways for diversity-oriented clicking. Together, these features support rapid functionalization and efficient access to structurally diverse analogs, offering a versatile platform for expansion of chemical space geared towards the development of bioactive molecules.

Introduction

Pyrazoles, a class of five-membered nitrogen-containing heterocycles, are valued for their structural versatility and broad applicability in synthetic organic chemistry.[1,2] Their ability to engage in hydrogen bonding, π-stacking, and metal coordination has made them indispensable in medicinal chemistry, agrochemicals, and materials science.[3–7] Pyrazole motifs are present in numerous pharmaceuticals, dyes, metal complexes, and supramolecular systems, highlighting their role as privileged scaffolds in molecular design.[7–16] Their prevalence across diverse fields reflects not only their synthetic accessibility but also their adaptability to a wide range of functionalization strategies and biological targets.[17,18]

Among its derivatives, fluorinated pyrazoles have garnered significant attention for their enhanced pharmacological properties.[14,15] The unique characteristics of fluorine, such as high electronegativity, small atomic radius, and strong carbon–fluorine bond,[19,20] can significantly improve metabolic stability, lipophilicity, and target binding affinity.[21–24] These attributes make fluorinated pyrazoles valuable in drug discovery,[25–27] agrochemistry,[28] and as ligands in coordination and organometallic chemistry (Fig. 1).[29–32]

Fluorinated pyrazoles remain a focal point of research across multiple scientific domains as a result of their unique characteristics and broad applicability. As such, the design and synthesis of structurally diverse, selectively fluorinated

pyrazoles remain a critical strategy for modulating reactivity, tuning physicochemical properties, and enabling targeted applications. Due to our interest in the electronic tuning of 1,3-dipolar cycloadditions through the incorporation of fluorine and other heteroatoms,[33–45] we sought to generate a fluorinated pyrazole containing a SuFEx-able handle for diversity-oriented click strategies.[46–48] As a robust and orthogonal click transformation, SuFEx offers a reliable platform to enable modular diversification.[49–54]

Herein, we report a rapid synthesis of 5-(trifluoromethyl)-1*H*-pyrazole-3-sulfonyl fluoride, a novel fluorinated pyrazole, through a mild 1,3-dipolar cycloaddition between 2,2,2-trifluorodiazoethane and 1-bromoethene-1-sulfonyl fluoride (Br-ESF). This scaffold is structurally significant, containing the sulfonyl fluoride as a clickable reactive handle, as well as the trifluoromethyl group (CF_3) and the pyrazole ring—pharmacophores frequently found in bioactive molecules (Scheme 1).[55–57] The presence of these motifs within a single framework highlights their potential relevance in drug discovery.

Results and discussion

Synthesis of a SuFEx-able trifluoromethylated pyrazole

The synthesis of the SuFEx-able fluorinated pyrazole harnessed the *in situ* generation of 2,2,2-trifluorodiazoethane due to its known propensity to react violently.[29,58,59] Initial attempts focused on conditions we reported previously for the 1,3-dipolar cycloadditions stabilized diazoacetates and diazoacetamides with Br-ESF.[46,48] Combining 2,2,2-trifluoroethan-1-amine hydrochloride **1**, sodium nitrite, and Br-ESF **2** in methylene chloride in one pot failed to yield the desired product. Varying the order of addition—first reacting the amine salt **1** with

[a]Department of Chemistry and Biochemistry, New Mexico State University, Las Cruces, New Mexico, 88003, USA. E-mail: bgold@nmsu.edu

[b]Computational Chemistry Laboratory, Department of Chemistry, Central Luzon State University, Science City of Muñoz, Nueva Ecija, 3120, Philippines
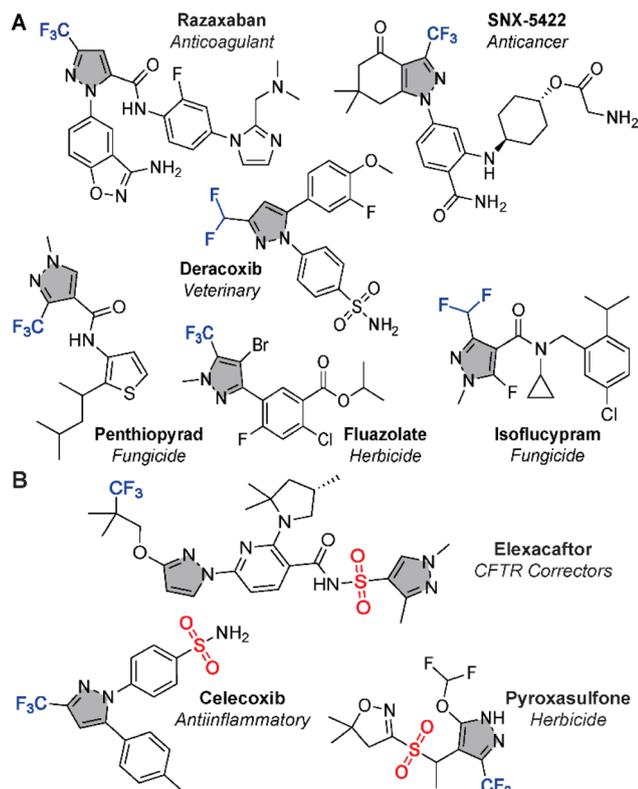
Fig. 1 (A) Commercially available bioactive compounds with fluorinated pyrazole motifs in their structures. (B) Examples of bioactive compounds containing all three motifs: CF$_3$, pyrazole, and sulfonyl group.

sodium nitrite in DCM, followed by the addition of Br-ESF **2**—also proved unsuccessful, with no product detected after 2 or 12 hours (Table 1, entries 1 and 2). Additionally, changing the solvent to acetonitrile or using excess sodium nitrite in DCM had no significant effect (entries 3 and 4). The 1,3-dipolar cycloaddition reaction of *in situ* generated trifluorodiazoethane **3** with Br-ESF required modification of the conditions we previously reported.[46,48]

A new product formed when a small amount of water was added to the reaction mixture, as determined by thin-layer chromatography. This finding suggested that the desired pyrazole **4** could be forming, which was later confirmed by the retention factor upon isolation. Based on this observation, we employed a biphasic solvent system of toluene and water (5 : 1)
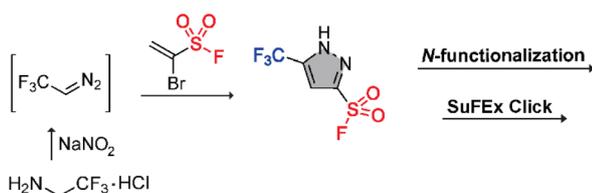
Scheme 1 Our strategy for the synthesis of SuFEx-able fluorinated pyrazole *via* 1,3-dipolar cycloaddition of diazo derivative with Br-ESF and subsequent diversification.

and increased the equivalents of diazo precursor **1** and NaNO$_2$ (relative to Br-ESF **2**). We also separated the organic phase from the aqueous phase and dried it over magnesium sulfate prior to the introduction of Br-ESF **2**. Under these optimized conditions, the reaction yielded 72% after 12 hours (entry 6). In contrast, using equal quantities of starting materials (**1** and NaNO$_2$) in the biphasic solvent resulted in a drop in yield (entry 7), highlighting the importance of reagent stoichiometry and solvent composition. The optimized overall yield is similar to that found for stabilized diazo compounds with Br-ESF **2**,[46,48] suggesting efficient formation of trifluorodiazoethane **3**.

Computational analysis

Insights into the 1,3-dipolar cycloaddition reactivity of the CF$_3$-substituted diazo compound (CF$_3$-diazo) were provided by DFT calculations. Geometry optimizations of ground state and transition state structures were performed using Gaussian 16 at the M06-2X/6-31G(d) level of theory, followed by single-point energy calculations at the M06-2X/6-311++G(d,p) level of theory with a PCM solvation model for toluene.[60,61] The reaction with Br-ESF was compared against *N*-methyldiazoacetamide (NMe-diazo) and methyl diazoacetate (OMe-diazo)—simplified models of two synthetically useful dipoles also bearing electron-withdrawing substituents.[36,44,46,62,63] We focused on stereo-electronic factors contributing to their reactivities throughout the reaction coordinate,[35,45,62,64] as well as the energetic trade-off of molecular distortions during bond formation.[65]

Despite possessing a lower-energy HOMO—which would typically disfavor a normal electron demand (NED) pathway—CF$_3$-diazo ($\Delta E^{\ddagger} = 7.9$ kcal mol^{-1}) undergoes the cycloaddition with Br-ESF more readily than NMe-diazo ($\Delta E^{\ddagger} = 9.6$ kcal mol^{-1}) and OMe-diazo (11.7 kcal mol^{-1}). This counterintuitive reactivity trend suggests that electronic effects beyond the primary HOMO–LUMO interaction play a critical role.

To elucidate the origin of the increased cycloaddition reactivity of the CF$_3$-diazo relative to the conjugated diazo compounds, we performed detailed distortion–interaction (DI) analysis throughout the intrinsic reaction coordinate (IRC),[65] and Natural Bond Orbital (NBO) analysis.[66]

Distortion–interaction (DI)/strain–activation analysis.. DI analysis provides a computational framework for dissecting (1,3-dipolar cycloaddition) reactivity by quantifying the energetic cost of distorting the reactants in isolation ($\Delta E^{\ddagger}_{\text{dist}}$ or $\Delta E^{\ddagger}_{\text{strain}}$), which is offset by stabilizing interaction energies ($\Delta E^{\ddagger}_{\text{interaction}}$) between reactants as the reaction proceeds.[65] Previous studies attribute relative cycloaddition reactivity to the differences in distortion energies of the 1,3-dipole.[67,68] Consistent with this, comparison of distortion energies highlights a distinct difference for the CF$_3$-substituted diazo (Fig. 2A). At the TS, the CF$_3$-diazo exhibits the lowest overall distortion energy ($\Delta E^{\ddagger}_{\text{dist}} = 21.6$ kcal mol^{-1}; diazo: 13.4 kcal mol^{-1}, Br-ESF: 8.2 kcal mol^{-1}), whereas NMe- and OMe-diazo require significantly higher total distortion energies (25.9 and 26.8 kcal mol^{-1}, respectively). Geometrically, this reduction results from a less strained diazo group in CF$_3$-diazo, as indicated by its ~1.5° larger bond angle relative to NMe- and OMe-diazos. These

Table 1 Optimization of reaction conditions for the synthesis of 5-(trifluoromethyl)-1H-pyrazole-3-sulfonyl fluoride
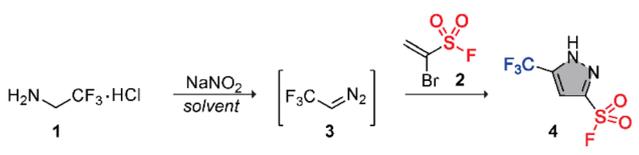
Entry	**1** (equiv.)	NaNO$_2$ (equiv.)	**4** (equiv.)	Solvent	t, h	Yield[a], %
1	0.9	0.9	1.0	DCM	2	—
2	0.9	0.9	1.0	DCM	12	—
3	0.9	0.9	1.0	MeCN	12	—
4	3.0	5.0	1.0	DCM	2	—
5	3.0	5.0	1.0	DCM/H$_2$O	12	Trace[b]
6	**6.0**	**10.0**	**1.0**	**Toluene/H$_2$O**	**12**	**72**
7	2.0	2.0	1.0	Toluene/H$_2$O	12	53

[a] Isolated yield, unless otherwise stated. [b] Determined by TLC.

trends are expected due to the relatively weaker hyperconjugative $n_C \to \sigma^*_{C-F}$ *versus* $n_C \to \pi^*_{C|O}$ interactions in the acetamide and acetate. While such differences at the TS are well established, a fuller picture requires examining how strain/activation energies evolve along the IRC to reveal the trajectory of structural and electronic adjustments leading to the TS.

In parallel, analysis of the interaction component reveals an important trade-off: CF$_3$-diazo exhibits the least stabilizing interaction energy ($\Delta E^{\ddagger}_{interaction} = -13.7$ kcal mol^{-1}) among the three models. The reduced distortion cost offsets this weaker stabilization, aligning with the previous findings where activation energy is governed not solely by interaction strength but by the energetic feasibility of achieving the TS geometry.[65,69–71] This balance reflects the nature of the CF$_3$-diazo system—weaker interactions are compensated by the formation of new bonds at an earlier stage in the reaction, leading to an earlier TS (*vide infra*).

The enthalpy (ΔH) profiles reveal the presence of pre-reaction complexes for all diazo systems (Fig. S2).[72] Both NMe- and OMe-diazo form slightly deeper enthalpic wells ($\Delta H = -9.5$ and -7.2 kcal mol^{-1}) than CF$_3$-diazo (-4.5 kcal mol^{-1}).

Additionally, their geometries are less aligned with the transition state, leading to greater reorganization during bond formation. In contrast, the CF$_3$-diazo pre-complex is geometrically pre-organized along the reaction coordinate, positioning the reacting centres of the diazo and Br-ESF moieties in a near-TS orientation. This improved preorganization reduces the translational and rotational adjustments required to reach the TS, lowering the effective distortion energy and contributing to the smaller pre-complex → TS enthalpic gap observed for CF$_3$-diazo. Together, these features rationalize its enhanced cycloaddition reactivity relative to the more stabilized yet less efficiently oriented NMe- and OMe-diazo systems.

Intrinsic reaction coordinate (IRC) analysis. To examine how interaction and distortion energies evolve prior to the TS, we calculated the intrinsic reaction coordinate (IRC) profiles[69] for all the systems (Fig. 2B). At a consistent forming-bond length (~2.27 Å), all systems have similar distortion energies (CF$_3$-diazo: 21.6 kcal mol^{-1}, NMe-diazo: 20.9 kcal mol^{-1}, OMe-diazo: 22.7 kcal mol^{-1}); however, interaction energies differed more significantly, with CF$_3$-diazo showing the strongest stabilizing value (-13.7 kcal mol^{-1}). Strain energies accumulate similarly
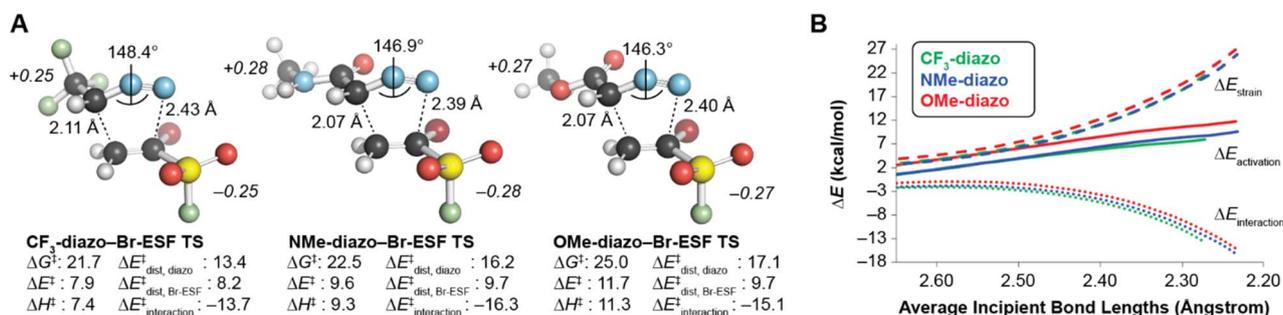

Fig. 2 Computational analysis for the 1,3-dipolar cycloaddition transition state between diazo compounds (CF$_3$-diazo, NMe-diazo, OMe-diazo) and Br-ESF performed at the M06-2X/6-311++G(d,p)-PCM(toluene)//M06-2x/6-31G(d) level of theory. (A) Optimized transition state geometries, NBO charges (italics), free energies of activation (kcal mol^{-1}), and distortion–interaction (strain–activation) analysis. (B) Distortion–interaction (strain–activation) analysis along the intrinsic reaction coordinate.

across the system, but the more favorable early-stage interaction in CF$_3$-diazo indicates a better preorganization or early-stage orbital alignment, allowing the system to cross the intrinsic barrier earlier along the reaction coordinate. In line with Hammond's postulate,[73] the more exergonic cycloaddition of CF$_3$-diazo ($\Delta G = -18.0$ kcal mol^{-1}) correlates with an earlier, less distorted TS, compared to the NMe- (-14.3 kcal mol^{-1}) and OMe-diazo dipoles (-9.6 kcal mol^{-1}; Table S1).[34,40,70,74] Thus, the apparent trade-off between weaker stabilizing interactions at the TS and lower activation energies arises because bond formation is initiated sooner, thereby reducing the distortion penalty. Overall, reactivity is modulated not only by the magnitude of strain or interaction but also by the timing and the efficiency of their buildup along the reaction coordinate.

Insights into the origin of the interaction energy were obtained by examining charge transfer between reactants using NBO charges, electrostatic interactions from Coulombic energies between the vinylic hydrogen of Br-ESF and the diazo substituent's heteroatoms, and steric exchange from interactions between Br lone pairs and either the F lone pairs (CF$_3$-diazo) or the carbonyl π orbitals (NMe- and OMe-diazo) at a consistent forming-bond length ($\sim$2.27 Å; Fig. S3 and Table S3). Charge transfer was similar across the series, indicating minimal differences in orbital interactions. In contrast, electrostatic stabilization decreased significantly for CF$_3$-diazo ($E_{ES} = 23.0$ kcal mol^{-1}) compared to NMe- and OMe-diazo (35.1 and 31.8 kcal mol^{-1}, respectively), consistent with the reduced dipolar character. The steric (Pauli) component exhibited the opposite trend, with CF$_3$-diazo exhibiting slightly higher steric energy ($E_{steric} = 1.4$ kcal mol^{-1}) than NMe- and OMe-diazo (≈ 0.4 kcal mol^{-1}), reflecting a closer Br–F distance in the TS. Overall, the reduced $\Delta E_{interaction}$ of CF$_3$-diazo arises primarily from weaker electrostatic stabilization rather than differences in charge transfer, and the enhanced cycloaddition reactivity is driven by minimized distortion.

Frontier molecular orbitals (FMO) and natural bond orbital (NBO) analysis. The cycloadditions proceed *via* an NED pathway—where the HOMO of the diazo compound donates into the LUMO of Br-ESF.[10,15] However, the observed reactivity trend (CF$_3$-diazo > NMe-diazo > OMe-diazo) is not fully explained by HOMO–LUMO energy gaps alone (Fig. 3A). Although CF$_3$-diazo shows the highest reactivity, its HOMO–LUMO gap with Br-ESF is relatively large. Instead, secondary orbital interactions and electronic delocalization, revealed by NBO analysis,[66] provide a clearer explanation.

NBO analysis highlights the role of intramolecular stabilization and reorganization across the diazo dipoles. In CF$_3$-diazo, strong n$_C \rightarrow \sigma^*_{CF}$ hyperconjugation (39.0 kcal mol^{-1} in the SM) weakens significantly at the TS (25.6 kcal mol^{-1}), consistent with early polarization and reorganization. Simultaneously, the n$_C \rightarrow \pi^*_{NN}$ delocalization (234.2 kcal mol^{-1} in SM) diminishes significantly at the TS (135.1 kcal mol^{-1}), indicating substantial lone pair redistribution that facilitates new bond formation (Fig. 3B). In contrast, NMe- and OMe-diazo are dominated by strong n$_C \rightarrow \pi^*_{C]O}$ delocalization in the SM (87.3 and 95.3 kcal mol^{-1}, respectively), which diminishes quickly at the TS (51.2 and 57.4 kcal mol^{-1}), increasing their reorganization
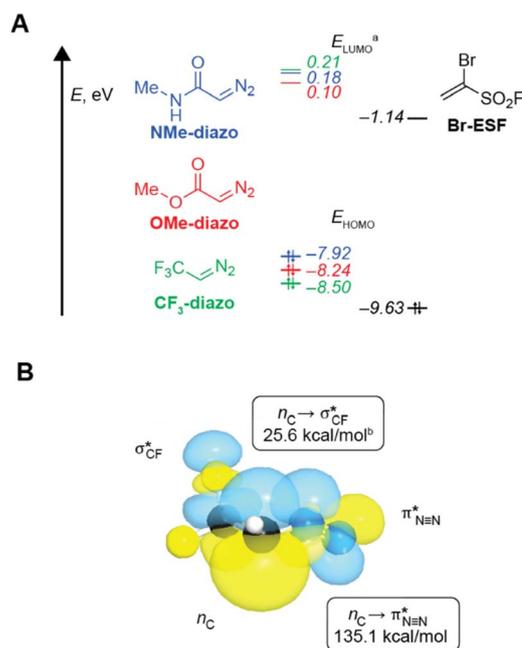

Fig. 3 CF$_3$-diazo harnesses secondary orbital interactions to accelerate cycloaddition reaction with Br-ESF. (A) Frontier molecular orbital energies, and (B) stereoelectronic interactions in the CF$_3$-diazo during its cycloaddition with Br-ESF, calculated at M06-2X/6-311++G(d,p)-PCM(toluene) level of theory. ^{a}Energies correspond to the LUMO+1 of OMe-diazo and the LUMO+2 of NMe- and CF$_3$-diazo (see: Fig. S1). ^{b}Sum of n$_C \rightarrow \sigma^*_{CF}$ interaction energies.

penalty. Their n$_C \rightarrow \pi^*_{NN}$ interactions, while substantial, are slightly weaker at the TS (132.0 and 128.9 kcal mol^{-1}) compared to CF$_3$-diazo (Table S2).

Altogether, the CF$_3$-group reduces the reorganization penalty by limiting the loss of stabilizing interactions while maintaining strong delocalization within the diazo moiety. Thus, while HOMO–LUMO overlap defines the primary interaction in this NED pathway, the enhanced reactivity of CF$_3$-diazo originates from stereoelectronic effects: ground-state σ_{CF} hyperconjugation that is traded off with minimal energetic cost, combined with efficient electron density redistribution into π_{NN} delocalization at the TS. These features lower the energetic penalty required to distort the CF$_3$-diazo and stabilize an earlier TS, resulting in an acceleration of the cycloaddition beyond what FMO gaps alone would predict.

SuFEx-based derivatization

We next explored the scope of nucleophiles compatible with this fluorinated pyrazolyl SuFEx hub using previously optimized conditions.[46,75] We began by evaluating various nitrogen-containing nucleophiles, which readily afforded the corresponding sulfonamides (Fig. 4). When 5-(trifluoromethyl)-1H-pyrazole-3-sulfonyl fluoride 4 was reacted with aniline in the presence of DABCO as a base and Ca(NTf$_2$)$_2$ as an additive, efficient substitution at the sulfur(VI)–fluoride bond afforded sulfonamide 5a in excellent yield. Similarly, substituted aryl-amines and benzylamine underwent smooth conversion to the
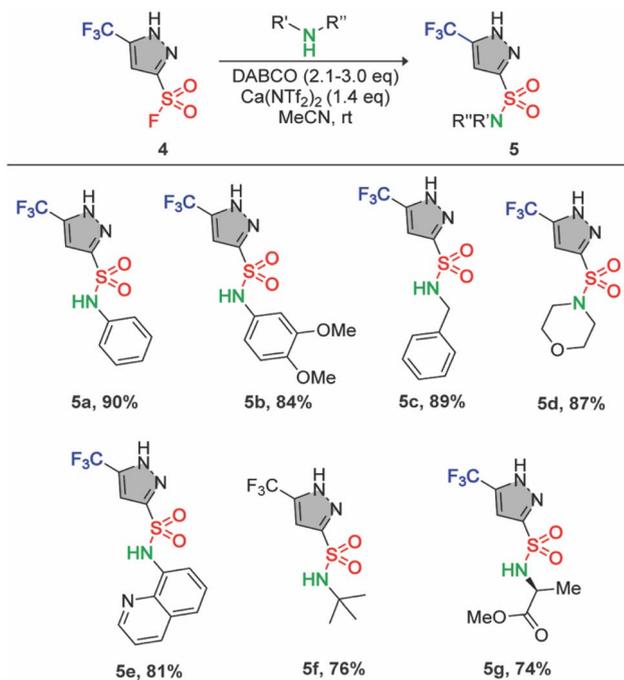
Fig. 4 Synthesis of pyrazolyl sulfonamides *via* SuFEx reaction, illustrating the scope of the reported fluorinated SuFEx-able pyrazole.

Fig. 5 Synthesis of pyrazolyl sulfonates *via* SuFEx reaction, illustrating the scope of the reported fluorinated SuFEx-able pyrazole.

corresponding sulfonamides **5b** and **5c** under identical conditions. Morpholine, a representative secondary amine, also delivered the expected sulfonamide product in excellent yield. In addition, aliphatic amines were found to be viable partners in this SuFEx transformation. For example, *tert*-butylamine reacted with compound **4** to afford sulfonamide **5f** in 76% yield. To further highlight the applicability of this method to biologically relevant substrates, we reacted an amino acid derivative, which furnished the desired sulfonamide product **5g** in 74% yield.

We also explored the reactivity of oxygen-containing nucleophiles with the SuFEx-able fluorinated pyrazole **4**. Substituted aryl alcohols underwent SuFEx reactions efficiently at room temperature, providing the corresponding aryl sulfonates (**6a–e**) in excellent yields (Fig. 5). Similarly, the heteroaromatic alcohol 2-methylpyridin-3-ol reacted smoothly with **4** to yield sulfonate **6f** in 81% yield. In contrast, representative aliphatic alcohols, including cyclohexanol, methanol, and *tert*-butyl alcohol, were largely unreactive under the standard conditions, with starting materials recovered. Attempts to enhance reactivity by increasing the reaction temperature or adding excess base and additive did not result in product formation.

Intermolecular C–N coupling

After evaluating the effectiveness of SuFEx chemistry with various nucleophiles, we turned our attention to the *N*-functionalization of pyrazole (Fig. 6). Initially, we tested the *N*-alkylation of 5-(trifluoromethyl)-1*H*-pyrazole-3-sulfonyl fluoride **4** using benzyl bromide in the presence of various bases. While bases like triethylamine, diisopropylethylamine, and sodium
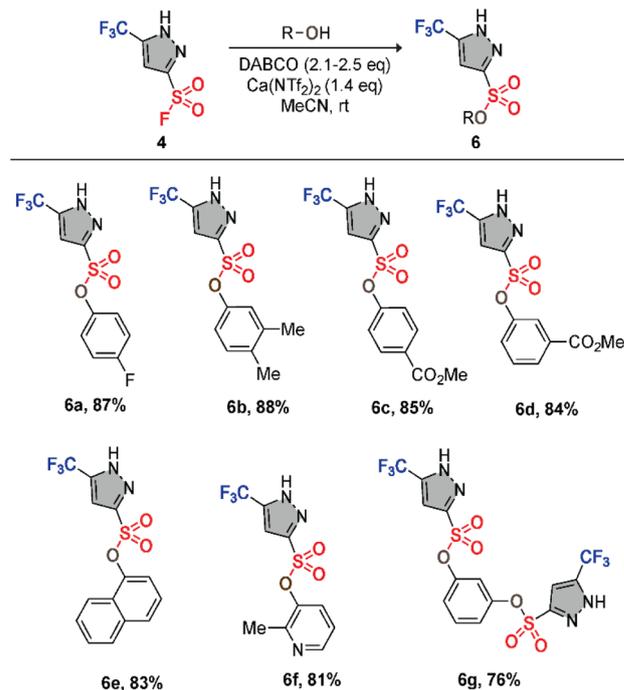
hydroxide proved ineffective, potassium carbonate (K_2CO_3) significantly improved the reaction, yielding high conversion and excellent isolated yields. DMSO was chosen as the solvent due to its ability to solvate larger alkali metal cations (such as K^+), as well as its high solubility for the reactants.[76,77] With the optimized conditions established, we explored *N*-substitution
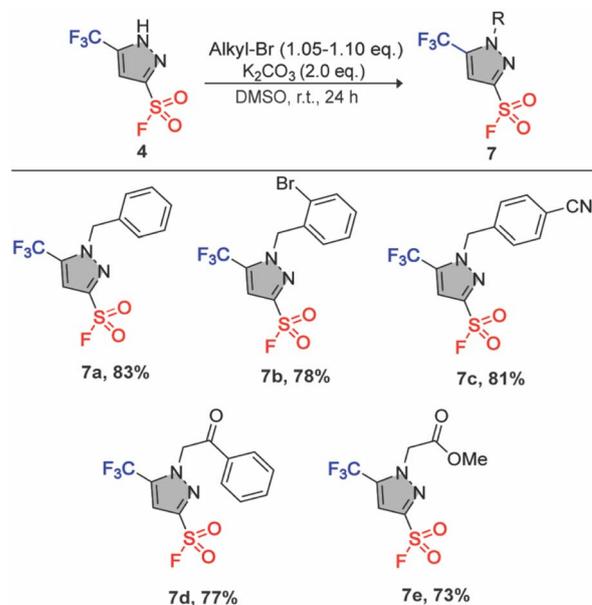

Fig. 6 *N*-alkylation of 5-(trifluoromethyl)-1*H*-pyrazole-3-sulfonyl fluoride with alkyl halides under basic conditions, affording *N*-alkylated products (**7a–e**).
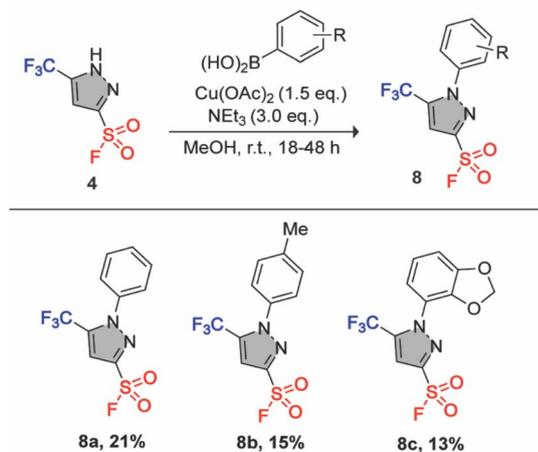
Paper

Fig. 7 Chan–Lam coupling of 5-(trifluoromethyl)-1*H*-pyrazole-3-sulfonyl fluoride with arylboronic acids afforded *N*-aryl products (**8a–c**) in low yields under mild conditions.

on the pyrazole scaffold using five representative substrates, obtaining consistently good yields (**7a–e**).

Following our success with *N*-alkylation, we sought to explore the intermolecular *N*-arylation of 5-(trifluoromethyl)-1*H*-pyrazole-3-sulfonyl fluoride as a route to further diversify the core scaffold. Initial attempts using Ullmann-type and Buchwald–Hartwig couplings proved ineffective, with minimal conversion and sluggish reactivity under standard conditions. Given the elevated temperatures and ligand-dependence typically required for these methods, we turned our attention to milder Chan–Lam-type couplings employing arylboronic acids.

Despite extensive screening (see Table S4), copper-mediated Chan–Lam conditions consistently afforded only low yields of the desired *N*-aryl products. The best outcome was observed using 1.5 equivalents of copper(II) acetate and excess triethylamine in methanol at room temperature, which furnished the *N*-arylated products in detectable but poor yields (Fig. 7). Three representative *N*-aryl derivatives (**8a–c**) were successfully isolated under these conditions, highlighting the generality of the transformation despite its limited efficiency. The lack of efficient reactivity likely stems from the combined effects of electron-withdrawing trifluoromethyl and sulfonyl fluoride substituents on the pyrazole ring, reducing the nucleophilicity of the nitrogen and altering its coordination behaviour. These findings suggest that the substrate presents intrinsic challenges under Chan–Lam-type conditions.

Conclusion

In conclusion, we have developed a concise and modular route to access 5-(trifluoromethyl)-1*H*-pyrazole-3-sulfonyl fluoride *via* a 1,3-dipolar cycloaddition between an *in situ*-generated diazo compound and Br-ESF. DFT and orbital analyses reveal that the exceptional 1,3-dipolar cycloaddition reactivity of CF$_3$-substituted diazo arises from its reduced distortion energy, early-stage orbital preorganization, and intramolecular

electronic reorganization, which together overcome a less favorable primary HOMO–LUMO interaction to enable an earlier, less strained transition state formation. Subsequent sulfur(VI) fluoride exchange (SuFEx) reactions with diverse nitrogen- and oxygen-based nucleophiles furnished the corresponding sulfonamides and sulfonates in good yields. Further functionalization of the pyrazole core was demonstrated through *N*-alkylation and *N*-arylation. *N*-alkylation proceeded efficiently under mild conditions, while *N*-arylation *via* Chan–Lam coupling led to low yields despite extensive optimization. These results highlight both the synthetic utility and current limitations of this scaffold, offering a foundation for future development of functionally diverse molecules with potential relevance in medicinal chemistry and materials science.

Experimental

1-Bromoethene-1-sulfonyl fluoride (Br-ESF) (2)

1-Bromoethene-1-sulfonyl fluoride (Br-ESF) (**2**) was prepared according to previously reported procedures.[53,78–80]

5-(Trifluoromethyl)-1*H*-pyrazole-3-sulfonyl fluoride (4)

In the mixture of water and the corresponding organic solvent (toluene), sodium nitrite (2.6 g, 10.0 equiv., 37.64 mmol) and 2,2,2-trifluoroethylamine hydrochloride (3.0 g, 6.0 equiv., 22.14 mmol) were added. The resulting mixture was stirred vigorously for 1 hour. Then, the organic layer was separated and dried over MgSO$_4$. To this layer, 1-bromoethene-1-sulfonyl fluoride (812 mg, 1.0 equiv., 3.69 mmol) was added and stirred overnight at room temperature. The solvent was evaporated, and the dry residue was fractioned upon silica and purified by flash chromatography eluting with hexane/EtOAc mixture 10 : 1 to afford the titled product 4 (1.16 g, 7.379 mmol, 72%) as a light-yellow oil. ^{1}H NMR (500 MHz, CDCl$_3$) δ 11.71 (br, 1H), 7.32 (s, 1H). ^{13}C {1H} NMR (126 MHz, CDCl$_3$) δ 143.2 (d, J = 37.6 Hz), 138.3 (d, J = 43.2 Hz), 119.0 (q, J = 270.2 Hz), 109.3. ^{19}F NMR (471 MHz, CDCl$_3$) δ 66.6, −61.1. HRMS (ESI-TOF) *m/z*: [M − H]$^-$ Calcd for C$_4$H$_2$F$_4$N$_2$O$_2$S 216.9701; found 216.9693.

General procedure for SuFEx

In a 3 mL vial, 5-(trifluoromethyl)-1*H*-pyrazole-3-sulfonyl fluoride 4 (1.0 equiv.), a nucleophile (1.0–1.1 equiv.), calcium bis((trifluoromethyl)sulfonyl)amide (1.4 equiv.), DABCO (2.1–3.0 equiv.), and 1 mL of acetonitrile were combined. The reaction was stirred at room temperature until the starting material was completely consumed, as confirmed by TLC. The solvent was removed under reduced pressure, and the resulting residue was dry loaded onto silica gel and purified by column chromatography using a hexanes/EtOAc mixture for elution. The titled product was obtained after further solvent removal under reduced pressure.

General procedure for *N*-alkylation

In a vial equipped with a magnetic stir bar, 5-(trifluoromethyl)-1*H*-pyrazole-3-sulfonyl fluoride 4 (1.0 equiv.), the corresponding alkyl bromide (1.05–1.1 equiv), and potassium carbonate (2.0

equiv.) were combined in DMSO (1 mL). The reaction mixture was stirred at 0 °C for 5–10 minutes, then allowed to warm to room temperature and stirred until complete consumption of the starting material, as monitored by TLC. The reaction was quenched with cold water and extracted with ethyl acetate. The organic layer, after drying over MgSO$_4$, was concentrated under reduced pressure. The resulting residue was dry loaded onto silica gel and purified by column chromatography using a hexane/EtOAc mixture for elution. The titled product was obtained after further solvent removal under reduced pressure.

General procedure for *N*-arylation

In a round-bottom flask containing MeOH, Cu(OAc)$_2$ (1.5 eq.) and NEt$_3$ (3.0 eq.) were added and stirred for 5–10 minutes. To this solution, 5-(trifluoromethyl)-1*H*-pyrazole-3-sulfonyl fluoride (1.0 eq.) was added and stirred for another 10 minutes. After 10 minutes, the corresponding aryl boronic acid (0.8 eq.) was added and stirred at room temperature (open flask) until completion. The reaction mixture was washed with water and extracted twice with ethyl acetate, dried over MgSO$_4$, and fractionated upon silica for purification *via* column chromatography using a mixture of ethyl acetate and hexanes. The titled product was obtained after further solvent removal under reduced pressure.

Author contributions

Bipin Khanal: conceptualization, experimental investigation, methodology, data curation, writing – review and editing; Mark Aldren M. Feliciano: computational investigation, writing – review and editing; Brian Gold: conceptualization, supervision, funding acquisition/project administration, data curation, writing – review and editing.

Conflicts of interest

There are no conflicts to declare.

Data availability

The data supporting this article have been included as part of the supplementary information (SI). Supplementary information: ^{1}H and ^{13}C NMR specta of synthesized compounds, together with their spectral data, as well as computational details, coordinates, and total energies. See DOI: https://doi.org/10.1039/d5ra07095c.

Acknowledgements

Notes and references

1 K. Karrouchi, S. Radi, Y. Ramli, J. Taoufik, Y. N. Mabkhot, F. A. Al-aizari and M. Ansar, Synthesis and Pharmacological Activities of Pyrazole Derivatives: A Review, *Mol. J. Synth. Chem. Nat. Prod. Chem.*, 2018, **23**, 134.

2 M. F. Khan, M. M. Alam, G. Verma, W. Akhtar, M. Akhter and M. Shaquiquzzaman, The therapeutic voyage of pyrazole and its analogs: A review, *Eur. J. Med. Chem.*, 2016, **120**, 170–201.

3 P. Yin, L. A. Mitchell, D. A. Parrish and J. M. Shreeve, Energetic N-Nitramino/N-Oxyl-Functionalized Pyrazoles with Versatile π–π Stacking: Structure–Property Relationships of High-Performance Energetic Materials, *Angew. Chem., Int. Ed.*, 2016, **55**, 14409–14411.

4 J. Portilla, Current Advances in Synthesis of Pyrazole Derivatives: An Approach Toward Energetic Materials, *J. Heterocycl. Chem.*, 2024, **61**, 2026–2039.

5 A. Secrieru, P. O'Neill and M. Cristiano, Revisiting the Structure and Chemistry of 3(5)-Substituted Pyrazoles, *Molecules*, 2019, **25**, 42.

6 G. Brewer, R. J. Butcher and P. Zavalij, Use of Pyrazole Hydrogen Bonding in Tripodal Complexes to Form Self Assembled Homochiral Dimers, *Materials*, 2020, **13**, 1595.

7 M.-C. Ríos and J. Portilla, Recent Advances in Synthesis and Properties of Pyrazoles, *Chemistry*, 2022, **4**, 940–968.

8 S. Nitu, M. S. Milea, S. Boran, G. Mosoarca, A. D. Zamfir, S. Popa and S. Funar-Timofei, Experimental and Computational Study of Novel Pyrazole Azo Dyes as Colored Materials for Light Color Paints, *Materials*, 2022, **15**, 5507.

9 H. F. Rizk, M. A. El-Badawi, S. A. Ibrahim and M. A. El-Borai, Synthesis of some novel heterocyclic dyes derived from pyrazole derivatives, *Arab. J. Chem.*, 2011, **4**, 37–44.

10 N. A. Daugherty and J. H. Swisher, Metal complexes of pyrazole, *Inorg. Chem.*, 1968, **7**, 1651–1653.

11 P. Devi, K. Singh and D. Makawana, Novel Pyrazole-Based Transition Metal Complexes: Spectral, Photophysical, Thermal and Biological Studies, *Chem. Biodivers.*, 2023, **20**, e202300072.

12 M. Viciano-Chumillas, S. Tanase, L. J. de Jongh and J. Reedijk, Coordination Versatility of Pyrazole-Based Ligands towards High-Nuclearity Transition-Metal and Rare-Earth Clusters, *Eur. J. Inorg. Chem.*, 2010, **2010**, 3403–3418.

13 J. Pérez and L. Riera, Pyrazole Complexes and Supramolecular Chemistry, *Eur. J. Inorg. Chem.*, 2009, **2009**, 4913–4925.

14 A. A. Stepanov, L. M. Gornostaev, S. F. Vasilevsky, E. V. Arnold, V. I. Mamatyuk, D. S. Fadeev, B. Gold and I. V. Alabugin, Chameleonic Reactivity of Vicinal Diazonium Salt of Acetylenyl-9,10-anthraquinones: Synthetic Application toward Two Heterocyclic Targets, *J. Org. Chem.*, 2011, **76**, 8737–8748.

15 A. Ojha, E. Das, X. Lin and B. Gold, Escape from Flatland: Pericyclic Reactions and Rearrangements of Diazofluorene with Biarylcyclooctynes for the Generation of Helicene-Like

Phenanthro-Pyrazoles, *Eur. J. Org Chem.*, 2025, **28**, e202500130.

16 S. F. Vasilevsky, B. Gold, T. F. Mikhailovskaya and I. V. Alabugin, Strain control in nucleophilic cyclizations: reversal of exo-selectivity in cyclizations of hydrazides of acetylenyl carboxylic acids by annealing to a pyrazole scaffold, *J. Phys. Org. Chem.*, 2012, **25**, 998–1005.

17 M.-C. Ríos and J. Portilla, Recent Advances in Synthesis and Properties of Pyrazoles, *Chemistry*, 2022, **4**, 940–968.

18 M. J. Naim, O. Alam, F. Nawaz, Md. J. Alam and P. Alam, Current status of pyrazole and its biological activities, *J. Pharm. Bioallied Sci.*, 2016, **8**, 2–17.

19 J. C. Sloop, C. Holder and M. Henary, Selective Incorporation of Fluorine in Pyrazoles, *Eur. J. Org Chem.*, 2015, **2015**, 3405–3422.

20 G. N. Lipunova, E. V. Nosova, V. N. Charushin and O. N. Chupakhin, Fluorine-containing pyrazoles and their condensed derivatives: Synthesis and biological activity, *J. Fluorine Chem.*, 2015, **175**, 84–109.

21 T. Yamazaki, T. Taguchi and I. Ojima, in *Fluorine in Medicinal Chemistry and Chemical Biology*, 2009, pp. 1–46.

22 E. Henary, S. Casa, T. L. Dost, J. C. Sloop and M. Henary, The Role of Small Molecules Containing Fluorine Atoms in Medicine and Imaging Applications, *Pharmaceuticals*, 2024, **17**, 281.

23 P. Shah and A. D. Westwell, The role of fluorine in medicinal chemistry: Review Article, *J. Enzyme Inhib. Med. Chem.*, 2007, **22**, 527–540.

24 A. Mendoza, Synthetic Approaches to Fluorinated Pharmaceuticals: Bioavailability and Target Specificity, *Res. Rev. J. Med. Org. Chem.*, 2024, **11**, 1–2.

25 M. L. Quan, P. Y. S. Lam, Q. Han, D. J. P. Pinto, M. Y. He, R. Li, C. D. Ellis, C. G. Clark, C. A. Teleha, J.-H. Sun, R. S. Alexander, S. Bai, J. M. Luettgen, R. M. Knabb, P. C. Wong and R. R. Wexler, Discovery of 1-(3'-Aminobenzisoxazol-5'-yl)-3-trifluoromethyl-N-[2-fluoro-4-[(2'-dimethylaminomethyl)imidazol-1-yl]phenyl]-1H-pyrazole-5-carboxyamide Hydrochloride (Razaxaban), a Highly Potent, Selective, and Orally Bioavailable Factor Xa Inhibitor, *J. Med. Chem.*, 2005, **48**, 1729–1744.

26 K. H. Huang, J. M. Veal, R. P. Fadden, J. W. Rice, J. Eaves, J.-P. Strachan, A. F. Barabasz, B. E. Foley, T. E. Barta, W. Ma, M. A. Silinski, M. Hu, J. M. Partridge, A. Scott, L. G. DuBois, T. Freed, P. M. Steed, A. J. Ommen, E. D. Smith, P. F. Hughes, A. R. Woodward, G. J. Hanson, W. S. McCall, C. J. Markworth, L. Hinkley, M. Jenks, L. Geng, M. Lewis, J. Otto, B. Pronk, K. Verleysen and S. E. Hall, Discovery of Novel 2-Aminobenzamide Inhibitors of Heat Shock Protein 90 as Potent, Selective and Orally Active Antitumor Agents, *J. Med. Chem.*, 2009, **52**, 4288–4305.

27 E. S. Roberts, K. A. Van Lare, B. R. Marable and W. F. Salminen, Safety and tolerability of 3-week and 6-month dosing of Deramaxx® (Deracoxib) chewable tablets in dogs, *J. Vet. Pharmacol. Ther.*, 2009, **32**, 329–337.

28 P. K. Mykhailiuk, Fluorinated Pyrazoles: From Synthesis to Applications, *Chem. Rev.*, 2021, **121**, 1670–1715.

29 P. K. Mykhailiuk, 2,2,2-Trifluorodiazoethane (CF3CHN2): A Long Journey since 1943, *Chem. Rev.*, 2020, **120**, 12718–12755.

30 A. A. Titov, O. A. Filippov, A. F. Smol'yakov, K. F. Baranova, E. M. Titova, A. A. Averin and E. S. Shubina, Dinuclear CuI and AgI Pyrazolates Supported with Tertiary Phosphines: Synthesis, Structures, and Photophysical Properties, *Eur. J. Inorg. Chem.*, 2019, **2019**, 821–827.

31 A. A. Titov, A. F. Smol'yakov, K. F. Baranova, O. A. Filippov and E. S. Shubina, Synthesis, structures and photophysical properties of phosphorus-containing silver 3,5-bis(trifluoromethyl)pyrazolates, *Mendeleev Commun.*, 2018, **28**, 387–389.

32 I. Bassanetti, C. Atzeri, D. A. Tinonin and L. Marchiò, Silver(I) and Thioether-bis(pyrazolyl)methane Ligands: The Correlation between Ligand Functionalization and Coordination Polymer Architecture, *Cryst. Growth Des.*, 2016, **16**, 3543–3552.

33 J. A. Codelli, J. M. Baskin, N. J. Agard and C. R. Bertozzi, Second-Generation Difluorinated Cyclooctynes for Copper-Free Click Chemistry, *J. Am. Chem. Soc.*, 2008, **130**, 11486–11493.

34 C. G. Gordon, J. L. Mackey, J. C. Jewett, E. M. Sletten, K. N. Houk and C. R. Bertozzi, Reactivity of Biarylazacyclooctynones in Copper-Free Click Chemistry, *J. Am. Chem. Soc.*, 2012, **134**, 9199–9208.

35 B. Gold, G. B. Dudley and I. V. Alabugin, Moderating Strain without Sacrificing Reactivity: Design of Fast and Tunable Noncatalyzed Alkyne–Azide Cycloadditions via Stereoelectronically Controlled Transition State Stabilization, *J. Am. Chem. Soc.*, 2013, **135**, 1558–1569.

36 E. G. Burke, B. Gold, T. T. Hoang, R. T. Raines and J. M. Schomaker, Fine-Tuning Strain and Electronic Activation of Strain-Promoted 1,3-Dipolar Cycloadditions with Endocyclic Sulfamates in SNO-OCTs, *J. Am. Chem. Soc.*, 2017, **139**, 8029–8037.

37 R. D. Bach, Ring Strain Energy in the Cyclooctyl System. The Effect of Strain Energy on [3 + 2] Cycloaddition Reactions with Azides, *J. Am. Chem. Soc.*, 2009, **131**, 5233–5243.

38 K. Chenoweth, D. Chenoweth and W. A. G. Iii, Cyclooctyne-based reagents for uncatalyzed click chemistry: A computational survey, *Org. Biomol. Chem.*, 2009, **7**, 5255–5258.

39 J. M. Dones, N. S. Abularrage, N. Khanal, B. Gold and R. T. Raines, Acceleration of 1,3-Dipolar Cycloadditions by Integration of Strain and Electronic Tuning, *J. Am. Chem. Soc.*, 2021, **143**, 9489–9497.

40 E. Das, M. A. M. Feliciano, P. Yamanushkin, X. Lin and B. Gold, Oxa-azabenzobenzocyclooctynes (O-ABCs): heterobiarylcyclooctynes bearing an endocyclic heteroatom, *Org. Biomol. Chem.*, 2023, **21**, 8857–8862.

41 M. J. Holzmann, N. Khanal, P. Yamanushkin and B. Gold, Remote Strain Activation in a Sulfate-Linked Dibenzocycloalkyne, *Org. Lett.*, 2023, **25**, 309–313.

42 N. A. Danilkina, A. I. Govdi, A. F. Khlebnikov, A. O. Tikhomirov, V. V. Sharoyko, A. A. Shtyrov, M. N. Ryazantsev, S. Bräse and I. A. Balova,

Heterocycloalkynes Fused to a Heterocyclic Core: Searching for an Island with Optimal Stability-Reactivity Balance, *J. Am. Chem. Soc.*, 2021, **143**, 16519–16537.

43 M. R. Aronoff, B. Gold and R. T. Raines, Rapid cycloaddition of a diazo group with an unstrained dipolarophile, *Tetrahedron Lett.*, 2016, **57**, 2347–2350.

44 B. Gold, M. R. Aronoff and R. T. Raines, 1,3-Dipolar Cycloaddition with Diazo Groups: Noncovalent Interactions Overwhelm Strain, *Org. Lett.*, 2016, **18**, 4466–4469.

45 B. Gold, N. E. Shevchenko, N. Bonus, G. B. Dudley and I. V. Alabugin, Selective Transition State Stabilization via Hyperconjugative and Conjugative Assistance: Stereoelectronic Concept for Copper-Free Click Chemistry, *J. Org. Chem.*, 2012, **77**, 75–89.

46 P. Yamanushkin, K. Kaya, M. A. M. Feliciano and B. Gold, SuFExable NH-Pyrazoles via 1,3-Dipolar Cycloadditions of Diazo Compounds with Bromoethenylsulfonyl Fluoride, *J. Org. Chem.*, 2022, **87**, 3868–3873.

47 Z. Wang, J. A. Homer, E. K. Zegeye, L. Dada, D. W. Wolan, S. Kitamura and J. E. Moses, Diversity oriented clicking for modular synthesis, *Nat. Rev. Methods Primer*, 2025, **5**, 52.

48 B. Khanal, K. Jaithum, M. A. M. Feliciano and B. Gold, Catalytic Ullmann-Type N-Arylation to Access Medicinally Important SuFEx-able Pyrazolo[1,5-a]Quinoxalinones, *Asian J. Org. Chem.*, 2025, **14**, e00474.

49 J. Dong, L. Krasnova, M. G. Finn and K. B. Sharpless, Sulfur(VI) Fluoride Exchange (SuFEx): Another Good Reaction for Click Chemistry, *Angew. Chem., Int. Ed.*, 2014, **53**, 9430–9448.

50 J. A. Homer, L. Xu, N. Kayambu, Q. Zheng, E. J. Choi, B. M. Kim, K. B. Sharpless, H. Zuilhof, J. Dong and J. E. Moses, Sulfur fluoride exchange, *Nat. Rev. Methods Primer*, 2023, **3**, 58.

51 Y. Chao, M. Subramaniam, K. Namitharan, Y. Zhu, V. Koolma, Z. Hao, S. Li, Y. Wang, I. Hudoynazarov, F. M. Miloserdov and H. Zuilhof, Synthesis of Large Macrocycles with Chiral Sulfur Centers via Enantiospecific SuFEx and SuPhenEx Click Reactions, *J. Org. Chem.*, 2023, **88**, 15658–15665.

52 J. S. Oakdale, L. Kwisnek and V. V. Fokin, Selective and Orthogonal Post-Polymerization Modification using Sulfur(VI) Fluoride Exchange (SuFEx) and Copper-Catalyzed Azide–Alkyne Cycloaddition (CuAAC) Reactions, *Macromolecules*, 2016, **49**, 4473–4479.

53 J. Thomas and V. V. Fokin, Regioselective Synthesis of Fluorosulfonyl 1,2,3-Triazoles from Bromovinylsulfonyl Fluoride, *Org. Lett.*, 2018, **20**, 3749–3752.

54 Y. Wang, Z. Hao, M. Islam, Y. Zhu, Y. Chao, S. P. Pujari, H. Zhao and H. Zuilhof, SuFEx Reactions When Shaken Not Stirred, *Adv. Synth. Catal.*, 2025, **367**, e70081.

55 S. M. Hoy, Elexacaftor/Ivacaftor/Tezacaftor: First Approval, *Drugs*, 2019, **79**, 2001–2007.

56 T. D. Penning, J. J. Talley, S. R. Bertenshaw, J. S. Carter, P. W. Collins, S. Docter, M. J. Graneto, L. F. Lee, J. W. Malecha, J. M. Miyashiro, R. S. Rogers, D. J. Rogier, S. S. Yu, G. D. Anderson, E. G. Burton, J. N. Cogburn,

S. A. Gregory, C. M. Koboldt, W. E. Perkins, K. Seibert, A. W. Veenhuizen, Y. Y. Zhang and P. C. Isakson, Synthesis and Biological Evaluation of the 1,5-Diarylpyrazole Class of Cyclooxygenase-2 Inhibitors: Identification of 4-[5-(4-Methylphenyl)-3-(trifluoromethyl)-1*H*-pyrazol-1-yl]benzenesulfonamide (SC-58635, Celecoxib), *J. Med. Chem.*, 1997, **40**, 1347–1365.

57 M. Nakatani, Y. Yamaji, H. Honda and Y. Uchida, Development of the novel pre-emergence herbicide pyroxasulfone, *J. Pestic. Sci.*, 2016, **41**, 107–112.

58 X. Zhang, Z. Liu, X. Yang, Y. Dong, M. Virelli, G. Zanoni, E. A. Anderson and X. Bi, Use of trifluoroacetaldehyde N-tfsylhydrazone as a trifluorodiazoethane surrogate and its synthetic applications, *Nat. Commun.*, 2019, **10**, 284.

59 R. Fields and J. P. Tomlinson, Reactions of 2,2,2-trifluorodiazoethane with carbon-nitrogen and carbon-oxygen multiple bonds, *J. Fluorine Chem.*, 1979, **14**, 19–28.

60 M. J. Frisch, G. W. Trucks, H. B. Schlegel, G. E. Scuseria, M. A. Robb, J. R. Cheeseman, G. Scalmani, V. Barone, G. A. Petersson, H. Nakatsuji, X. Li, M. Caricato, A. V. Marenich, J. Bloino, B. G. Janesko, R. Gomperts, B. Mennucci, H. P. Hratchian, J. V. Ortiz, A. F. Izmaylov, J. L. Sonnenberg, D. Williams-Young, F. Ding, F. Lipparini, F. Egidi, J. Goings, B. Peng, A. Petrone, T. Henderson, D. Ranasinghe, V. G. Zakrzewski, J. Gao, N. Rega, G. Zheng, W. Liang, M. Hada, M. Ehara, K. Toyota, R. Fukuda, J. Hasegawa, M. Ishida, T. Nakajima, Y. Honda, O. Kitao, H. Nakai, T. Vreven, K. Throssell, J. A. Montgomery jr, J. E. Peralta, F. Ogliaro, M. J. Bearpark, J. J. Heyd, E. N. Brothers, K. N. Kudin, V. N. Staroverov, T. A. Keith, R. Kobayashi, J. Normand, K. Raghavachari, A. P. Rendell, J. C. Burant, S. S. Iyengar, J. Tomasi, M. Cossi, J. M. Millam, M. Klene, C. Adamo, R. Cammi, J. W. Ochterski, R. L. Martin, K. Morokuma, O. Farkas, J. B. Foresman, and D. J. Fox, *Gaussian 16 Rev. C.01*, Wallingford, CT, 2016.

61 Y. Zhao and D. G. Truhlar, The M06 suite of density functionals for main group thermochemistry, thermochemical kinetics, noncovalent interactions, excited states, and transition elements: two new functionals and systematic testing of four M06-class functionals and 12 other functionals, *Theor. Chem. Acc.*, 2008, **120**, 215–241.

62 B. Gold, M. R. Aronoff and R. T. Raines, Decreasing Distortion Energies without Strain: Diazo-Selective 1,3-Dipolar Cycloadditions, *J. Org. Chem.*, 2016, **81**, 5998–6006.

63 M. R. Aronoff, B. Gold and R. T. Raines, 1,3-Dipolar Cycloadditions of Diazo Compounds in the Presence of Azides, *Org. Lett.*, 2016, **18**, 1538–1541.

64 I. V. Alabugin and B. Gold, in *Encyclopedia of Physical Organic Chemistry*, John Wiley & Sons, Ltd, 2017, pp. 1–93.

65 I. Fernández and F. M. Bickelhaupt, The activation strain model and molecular orbital theory: understanding and designing chemical reactions, *Chem. Soc. Rev.*, 2014, **43**, 4953–4967.

66 E. D. Glendening, J. Badenhoop, K. A. E. Reed, J. E. Carpenter, J. A. Bohmann, C. M. Morales, P. Karafiloglou, C. R. Landis and F. Weinhold, *NBO 7.0*,

Theoretical Chemistry Institute, University of Wisconsin, Madison, 2018.

67 B. Gold, M. R. Aronoff and R. T. Raines, Decreasing Distortion Energies without Strain: Diazo-Selective 1,3-Dipolar Cycloadditions, *J. Org. Chem.*, 2016, **81**, 5998–6006.

68 D. H. Ess and K. N. Houk, Distortion/Interaction Energy Control of 1,3-Dipolar Cycloaddition Reactivity, *J. Am. Chem. Soc.*, 2007, **129**, 10646–10647.

69 P. Vermeeren, S. C. C. van der Lubbe, C. Fonseca Guerra, F. M. Bickelhaupt and T. A. Hamlin, Understanding chemical reactivity using the activation strain model, *Nat. Protoc.*, 2020, **15**, 649–667.

70 D. H. Ess and K. N. Houk, Theory of 1,3-Dipolar Cycloadditions: Distortion/Interaction and Frontier Molecular Orbital Models, *J. Am. Chem. Soc.*, 2008, **130**, 10187–10198.

71 F. M. Bickelhaupt and K. N. Houk, Analyzing Reaction Rates with the Distortion/Interaction-Activation Strain Model, *Angew. Chem., Int. Ed.*, 2017, **56**, 10070–10086.

72 D. Loco, I. Chataigner, J.-P. Piquemal and R. Spezia, Efficient and Accurate Description of Diels-Alder Reactions Using Density Functional Theory, *ChemPhysChem*, 2022, **23**, e202200349.

73 G. S. Hammond, A Correlation of Reaction Rates, *J. Am. Chem. Soc.*, 1955, **77**, 334–338.

74 T. A. Hamlin, B. J. Levandowski, A. K. Narsaria, K. N. Houk and F. M. Bickelhaupt, Structural Distortion of Cycloalkynes Influences Cycloaddition Rates both by Strain

75 S. Mahapatra, C. P. Woroch, T. W. Butler, S. N. Carneiro, S. C. Kwan, S. R. Khasnavis, J. Gu, J. K. Dutra, B. C. Vetelino, J. Bellenger, C. W. am Ende and N. D. Ball, SuFEx Activation with Ca(NTf2)2: A Unified Strategy to Access Sulfamides, Sulfamates, and Sulfonamides from S(VI) Fluorides, *Org. Lett.*, 2020, **22**, 4389–4394.

76 A. Huang, K. Wo, S. Y. C. Lee, N. Kneitschel, J. Chang, K. Zhu, T. Mello, L. Bancroft, N. J. Norman and S.-L. Zheng, Regioselective Synthesis, NMR, and Crystallographic Analysis of N1-Substituted Pyrazoles, *J. Org. Chem.*, 2017, **82**, 8864–8872.

77 J. H. Exner and E. C. Steiner, Solvation and ion pairing of alkali-metal alkoxides in dimethyl sulfoxide. Conductometric studies, *J. Am. Chem. Soc.*, 1974, **96**, 1782–1787.

78 D. B. Eremin and V. V. Fokin, On-Water Selectivity Switch in Microdroplets in the 1,2,3-Triazole Synthesis from Bromoethenesulfonyl Fluoride, *J. Am. Chem. Soc.*, 2021, **143**, 18374–18379.

79 C. J. Smedley, M.-C. Giel, A. Molino, A. S. Barrow, D. J. D. Wilson and J. E. Moses, 1-Bromoethene-1-sulfonyl fluoride (BESF) is another good connective hub for SuFEx click chemistry, *Chem. Commun.*, 2018, **54**, 6020–6023.

80 J. Leng and H.-L. Qin, 1-Bromoethene-1-sulfonyl fluoride (1-Br-ESF), a new SuFEx clickable reagent, and its application for regioselective construction of 5-sulfonylfluoro isoxazoles, *Chem. Commun.*, 2018, **54**, 4477–4480.

and Interaction Energies, *Chem.–Eur. J.*, 2019, **25**, 6342–6348.